Restoring force model for circular RC columns strengthened by pre-stressed CFRP strips

Changdong Zhou [*1], Xilin Lu [2], Hui Li [1] and Teng Tian [1]

[1] *School of Civil Engineering, Beijing Jiaotong University, Beijing, 100044, China*
[2] *State Key Laboratory for Disaster Reduction in Civil Engineering, Tongji University, Shanghai, 200092, China*

Abstract. This paper presents a tri-linear restoring force model based on the test results of 12 circular RC columns strengthened by CFRP strips under low cyclic loading. The pre-stress of CFRP strips and axial load ratio of specimens are considered as the affect parameters of the proposed model. All essential characteristics of the hysteretic behavior of the proposed model, including the hysteretic rules, main performance points, strength degradation, stiffness degradation and confinement effects are explicitly analyzed. The calculated results from the proposed model are in good agreement with the experimental results, which shows that the recommended model can be reliably used for seismic behavior predictions of circular RC columns strengthened by pre-stressed CFRP strips.

Keywords: restoring force model; circular reinforced concrete column; pre-stressed fiber reinforced polymer; seismic behavior; active confinement

1. Introduction

Many reinforced concrete (RC) columns suffered serious damage in earthquakes which often results in the destruction of bridges and building structures. Bonding fiber reinforced polymer (FRP) has been commonly used to improve the seismic behavior of RC columns in practice (Xiao and Ma 1997, FIB 2001, ISIS 2001, JSCE 2001, Sheikh 2001, 2002; Teng *et al.* 2002, ACI 2008). Since the confinement in this case is a passive type, the confining stress is induced only after significant outward expansion of the core concrete is achieved (Burt and Aftab 1999). So the external FRP jacket has serious stress hysteresis, and pre-tensioning FRP can solve this problem. Previous studies have confirmed that the seismic behavior of concrete columns strengthened by pre-stressed FRP strips can be highly improved (Yamakawa *et al.* 2001, Nesheli and Meguro 2006, Taleie and Moghaddam 2007, Taleie and Oskouei 2007).

The restoring force refers to the ability to restore the deformation of the structures or components after external load is removed. While the restoring force characteristic is the relationship between the force and the displacement which can be described by the restoring force model. The restoring force model is important basis to analyze the seismic behavior of concrete columns (Stojadinovic and Thewalt 1996, Sivaselvan and Reinhorn 2000, Ibarra *et al.* 2005). The

---

∗Corresponding author, Professor, E-mail: zhouchangdong@163.com

low cyclic loading test is usually carried out to determine the restoring force model of concrete columns (Saatcioglu 1991).

The restoring force model for concrete columns has been presented for a long time (Tamai *et al*. 2000, Tao *et al*. 2005). But the lateral pre-stress isn't considered in these models, and the restoring force model for concrete columns strengthened by pre-stressed FRP has been rarely reported. To bridge this gap, the objective of the work reported here is to develop a tri-linear restoring force model including strength and stiffness deterioration properties for force-displacement response of circular RC columns strengthened with pre-stressed CFRP strips from lateral cyclic loading test data. The proposed restoring force model is based on the test results of 12 circular RC columns under lateral cyclic loading, and these specimens are strengthened by lateral pre-stressed CFRP strips. The axial load ratio and the lateral pre-stress of CFRP strips are considered as the main parameters in the proposed model.

2. Experimental program

2.1 Specimens design and the material properties

In this study, a total of 12 RC solid columns strengthened with pre-stress CFRP were prepared and subjected to low cyclic lateral loading and the constant axial compressive load. All the specimens were circular with diameter of 300 mm in cross section and 525 mm in height. Fig. 1 shows the details test setup and specimens. There are 8Φ22 longitudinal steel bars in C7, C10, C11 and C12, and 6Φ25 longitudinal steel bars in all other specimens. The material properties of concrete, steel bars and CFRP strips are listed in Table 1, where the concrete strength is the 28 day's test result after casting.

After the CFRP strips were pre-tensioned to the designed pre-stress, the constant axial load was imposed on the specimens, and then the lateral cyclic loads were beginning. Before the specimens
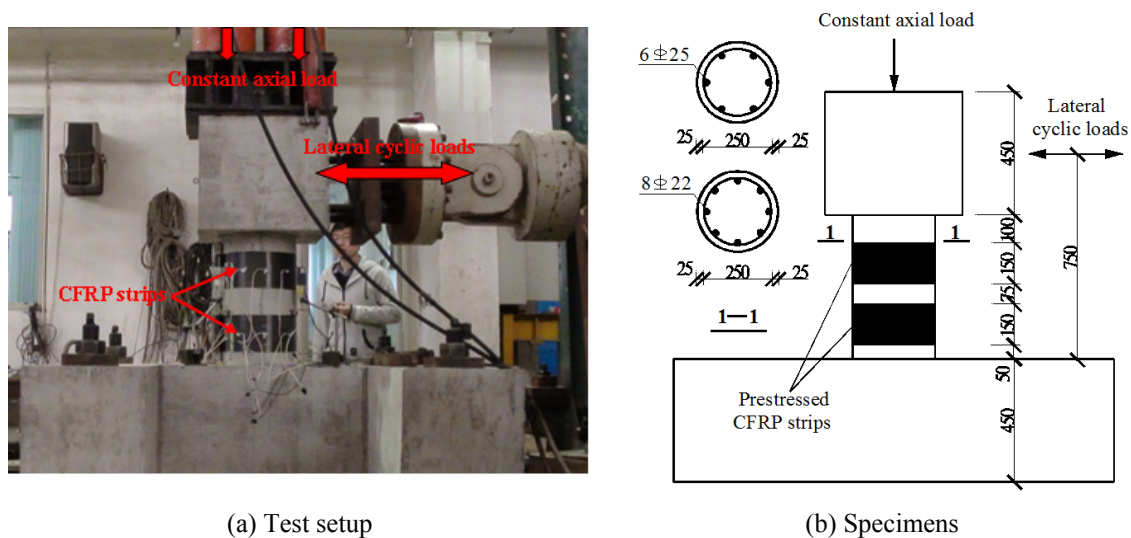

(a) Test setup   (b) Specimens

Fig. 1 Details of test setup and specimens

Table 1 Material properties

Material	Elastic Modulus GPa	Cube compressive strength of concrete MPa	Yield strength MPa	Ultimate tensile strength MPa	Ultimate strain	Thickness of each layer mm
C35	31.8	34.2	——	2.60	0.003	——
C40	32.6	40.6	——	2.90	0.003	——
$\phi6$	200	——	382	530	0.018	——
$\phi22$	200	——	350	532	0.017	——
$\phi25$	200	——	362	542	0.017	——
CFRP	241	——	——	3710	0.017	0.167

yielded, the lateral loading method was decided by the load, and the initial load increment was 30 kN. When the specimens nearly yielded, the load increment is changed into 5 kN. After the specimens yielded, the loading mode was transformed into displacement control, and the displacement increment is the yield displacement of specimens. At each control displacement, the specimens were loaded and unloaded for three times. The specimens damaged until the lateral load dropped to 85% of the peak load.

2.2 Test results and discussion

The characteristics and test results of specimens are listed in Table 2, where f_c is the cube compressive strength of concrete and it was obtained from compression tests on standard concrete cube in accordance with GB/T 50081-2002, unit: MPa; n is the axial compression ratio of specimens, and based the axial compression ratio, all the specimens are divided into two series: if the axial compression ratio is below or larger than 0.50; α is the pre-stress of CFRP strips, $\alpha = 0.10$ means the prestress of the CFRP strips is 0.10 times of its ultimate tensile strength; Δ_y and Δ_u is the yield displacement and ultimate displacement respectively, mm; P_m is the peak load, unit: kN; E is the total energy dissipation and it can be determined by integrating the areas bounded by the hysteretic loops, as shown in Fig. 3, unit: kN-mm. As seen from Table 2, the bearing capacity, deformation capacity, energy dissipation capacity and ductility of strengthened specimens are significantly improved.

The typical failure modes are illustrated in Fig. 2. As seen from Table 2 and Fig. 2, the failure modes of both un-strengthened specimens C1 and C7 belong to typical shear failure with poor ductility. With the help of pre-stressed CFRP strips, the failure modes of strengthened specimens change into bending failure with better ductility.

The hysteresis curves of specimens are shown in Fig. 3. As seen from Fig. 3 and Table 2, the hysteresis loops of strengthened specimens become well-rounded and less pinched, the energy dissipation capacity and plastic deformation capacity are greatly improved; there are apparent upper and lower intersection points of the hysteresis curves of strengthened specimens, almost all the rising curves pass the same point and is named as the upper intersection point, and almost all the decline curves pass another point and it is named as the lower point (Su 1998); the stiffness degradation in loading and unloading decreases with the pre-stress of CFRP strips increases; the strength degradation after peak load increases with the axial load ratio increases.

The backbone curves of specimens can be obtained by connecting the peak points of various

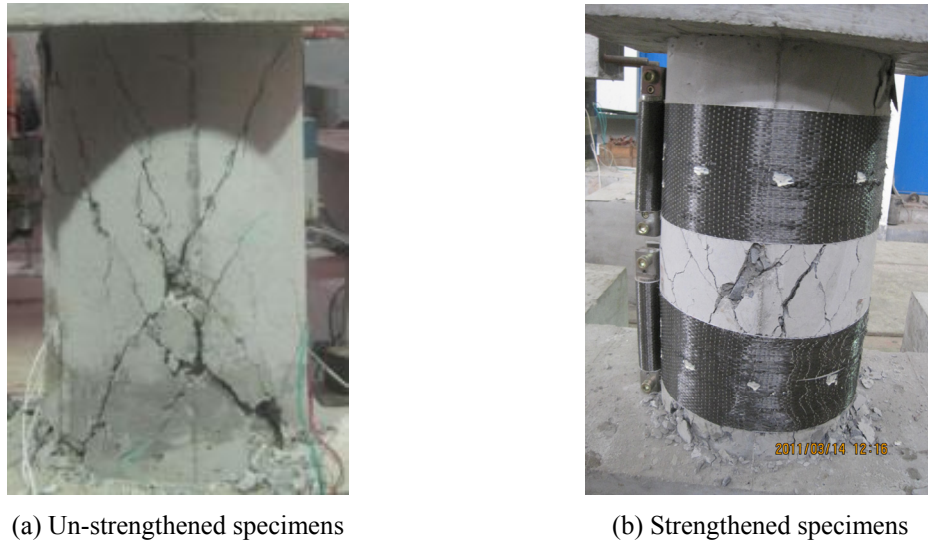(a) Un-strengthened specimens   (b) Strengthened specimens

Fig. 2 Typical failure modes for specimens

cyclic loading on the hysteresis curves of specimens which illustrated in Fig. 4. As seen from Fig. 4 and Table 2, the ductility increases with the pre-stress of CFRP strips increases; the lateral deformation capacity decreases with the axial load ratio increases. The backbone curves can be divided into three parts that are defined as elastic segment, strengthening segment and degradation segment. So the trilinear degradation curves (as seen from Fig. 5) can be better matched to the experimental results.

Table 2 Characteristics and test results of specimens

Specimen	f_c MPa	N	α	Failure mode	Δ_y mm	Δ_u mm	$\dfrac{\Delta_u}{\Delta_y}$	$\dfrac{\Delta_{ui}}{\Delta_{u1}}$	P_m kN	$\dfrac{P_{mi}}{P_{m1}}$	E kN-mm
C1	40.6	0.40	—	Shear	6.2	14.50	2.34	1.00	191.5	1.00	14740.80
C2	40.6	0.40	0	Bending	5.7	22.40	3.93	1.54	204.7	1.07	35526.54
C3	40.6	0.40	0.10	Bending	6.5	26.25	4.04	1.81	210.0	1.10	59357.28
C4	40.6	0.40	0.20	Bending	6.2	27.75	4.48	1.91	227.3	1.19	88979.59
C5	40.6	0.25	0.20	Bending	6.3	28.53	4.53	1.97	194.1	1.01	62873.62
C6	40.6	0.55	0.20	Bending	6.6	24.25	3.67	1.67	247.1	1.29	43409.27
C7	34.2	0.82	—	Shear	—	5.12	—	1.00	145.2	1.00	—
C8	40.6	0.55	0.25	Bending	6.3	24.21	3.84	1.67	235.2	1.23	59643.96
C9	34.2	0.70	0.10	Bending	6.2	21.34	3.44	4.17	207.1	1.43	41346.17
C10	34.2	0.70	0.20	Bending	5.9	23.11	3.92	4.58	210.8	1.45	39004.04
C11	34.2	0.82	0.10	Bending	6.1	17.41	2.85	3.40	218.2	1.50	19599.46
C12	34.2	0.82	0.20	Bending	6.0	19.22	3.20	3.75	213.1	1.47	27215.81

(a) C1

(b) C2

(c) C3

(d) C4

(e) C5

(f) C6

Fig. 3 Hysteresis curves of specimens

(g) C7

(h) C8

(i) C9

(j) C10

(l) C11

(m) C12

Fig. 3 Continued

(a) Specimens with lower axial load ratio

(b) Specimens with higher axial load ratio
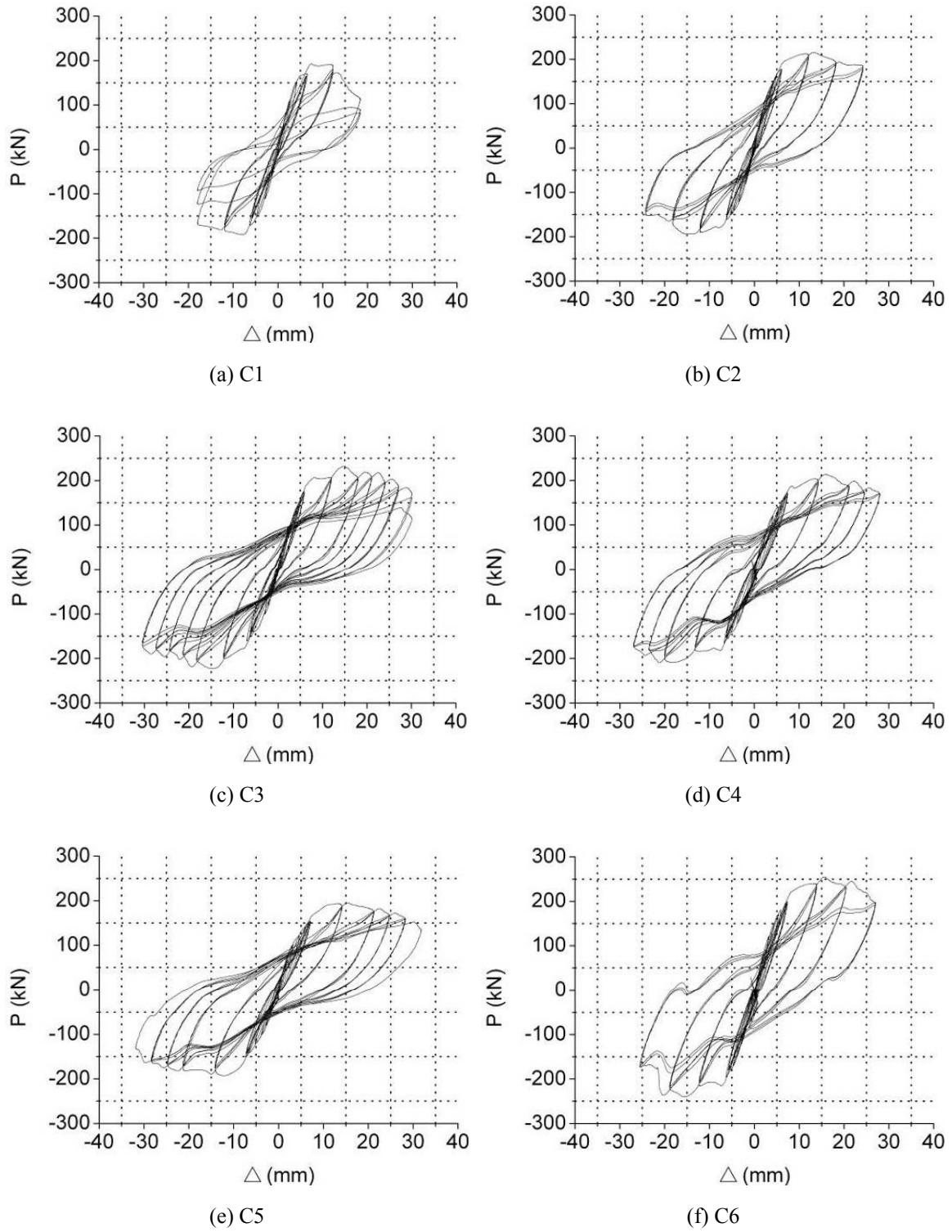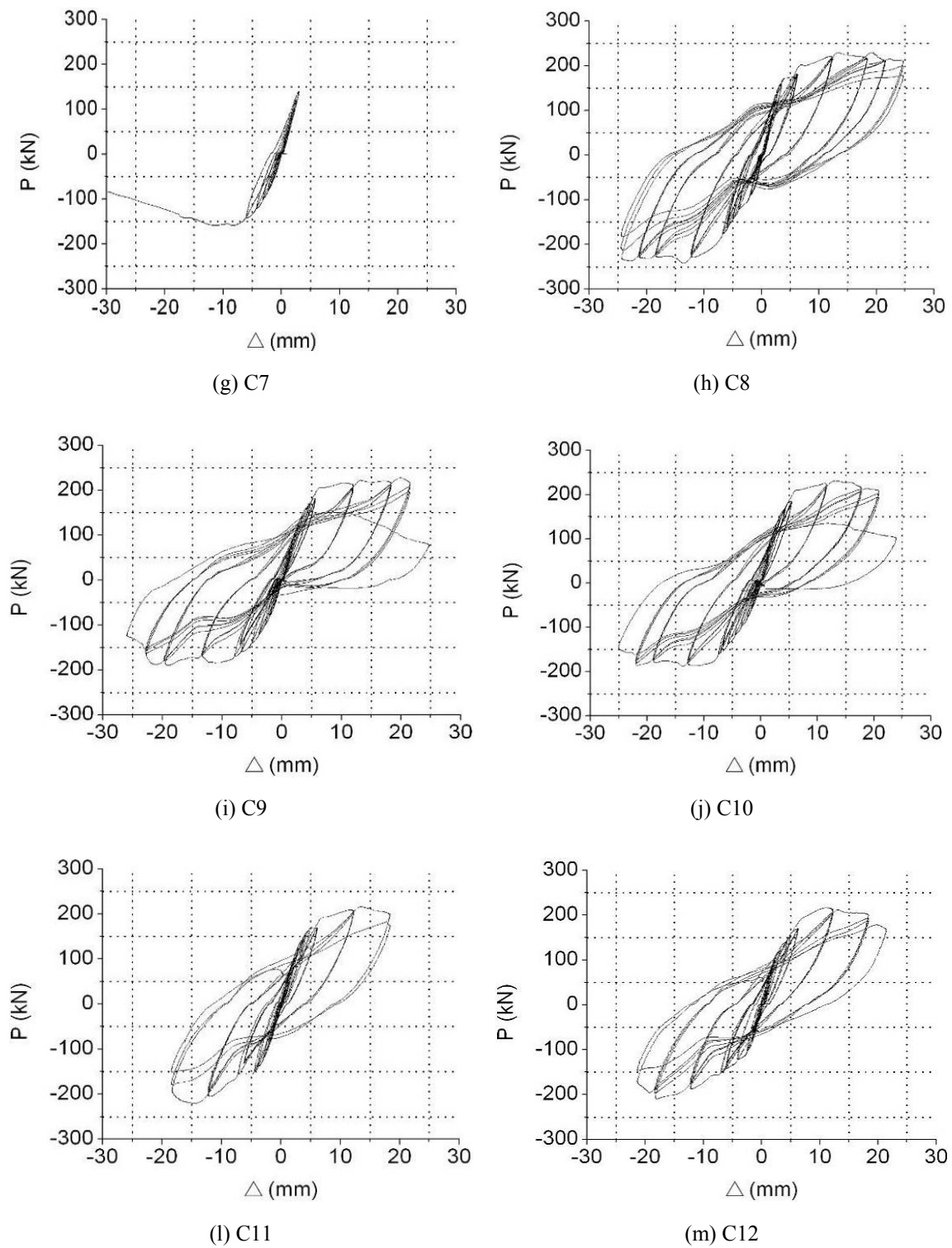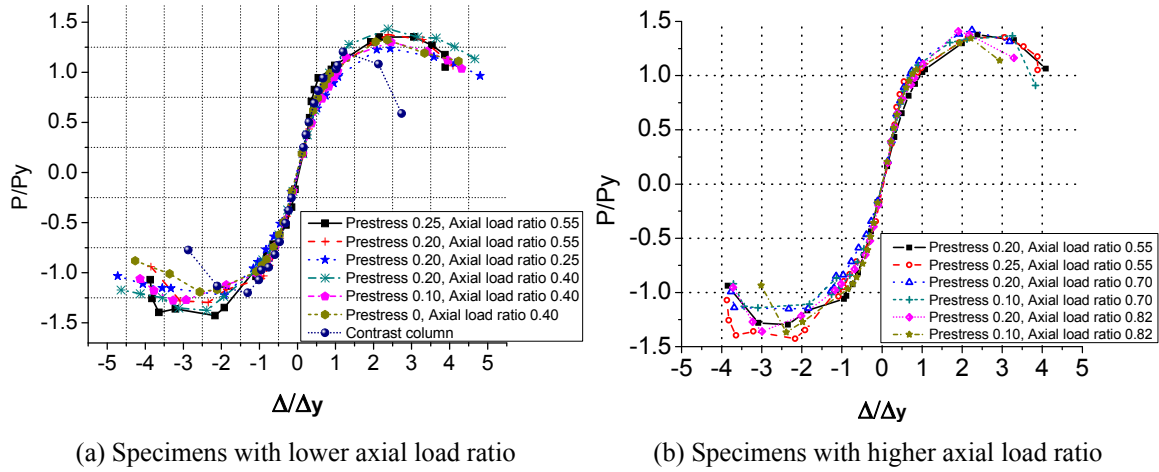
Fig. 4 Normalized backbone curves of specimens
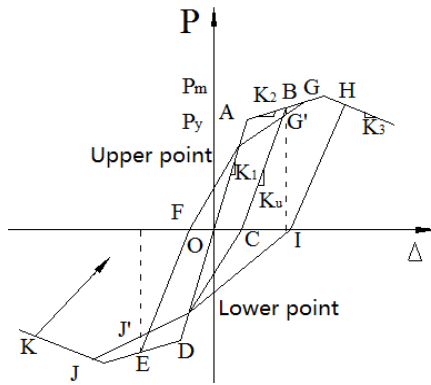

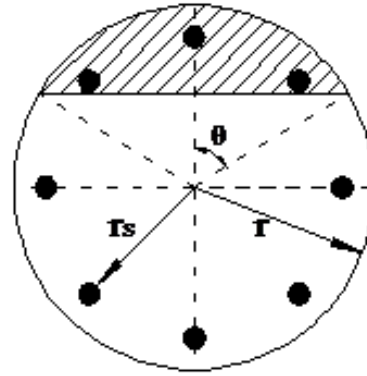Fig. 5 The restoring force model

Fig. 6 Cross-section of specimens

3. Restoring force model

The restoring force model represents the simplified relationship between the restoring force and the deformation, which summarizes the strength, stiffness, ductility and energy dissipation capacity of structures or components. The restoring force model includes backbone curves and hysteretic rules which is the basis of the structural elastic-plastic analysis (Stone and Taylor 1992, Stojadinovic and Thewalt 1996). As illustrated in Fig. 5, the key to determine the trilinear degradation model is to determine the following parameters: yield load P_y, yield displacement Δ_y, peak load P_m, peak displacement Δ_m, elastic stiffness K_1, strengthening stiffness K_2, degradation stiffness K_3 and unloading stiffness K_u. The nonlinear curve-fitting software 1st Opt is used to multiple nonlinear regression analysis of the experimental data.

3.1 The yield load P_y

Based on regression analysis of the experiment data, the yield load P_y can be calculated as

follows with considering the effect of the CFRP strips' pre-stress and the axial load ratio of specimens.

$$
P_y = \begin{cases} (1.43 - 2.66n + 3.05n^2 \\ -1.01\alpha + 1.1\alpha^2)P_m, & 0 < n < 0.55, \quad 0.1 < \alpha \le 0.25, \quad R = 0.9999 \\ \\ (-0.3 + 3.25n - 2.45n^2 \\ +0.38\alpha - 2\alpha^2)P_m, & 0.55 \le n \le 0.82, \quad 0.1 < \alpha \le 0.25, \quad R = 0.9955 \end{cases}
$$

(1)

where n is the axial load ratio, $n = N / f'_c A_g$, $0 \le n \le 0.82$; N is the design load; f'_c is the cylinder compressive strength of concrete, $f'_c = 0.8 f_c$ (CEB-FIP 1990); f_c is the cube compressive strength of concrete, and it has been listed in Table 1; A_g is the cross-sectional area of the specimens; a is the initial pre-stress of CFRP strips, $0.1 \le a \le 0.25$; P_m is the peak load of specimens, and it can be calculated as follows; R is the correlation coefficient in regression analysis.

3.2 The yield displacement Δ_y

The yield displacement Δ_y of specimens is significantly affected by the yield strain of longitudinal reinforcement and the cross-section diameter of specimens (Binici 2008). Based on the test results, the empirical formula of Δ_y can be expressed as follows

$$
\Delta_y = \frac{5.6 f_y l^2}{3 E_s D}
$$

(2)

where E_s and f_y are the elastic modulus and yield strength of the longitudinal reinforcement; l and D are the height and diameter of the specimens, respectively.

3.3 Peak load P_m

Based on the bearing capacity formula of circular RC columns strengthened with external bonding FRP jackets (Gu *et al.* 2010), the peak load (horizontal bearing capacity) P_m and the flexural bearing capacity M_u can be calculated as follows (Bai 2011)

$$
P_m = M_u / 0.75
$$

(3)

$$
M_u = f'_c \pi r^3 \times \left\{ \lambda'_l \left(1 - \frac{\theta}{\pi} \right) \left[\left(\frac{r_s}{r} \frac{\sin(\pi - \theta)}{\pi - \theta} \right) + \frac{4\sin^3\theta}{6\theta - 3\sin 2\theta} \right] + n' \frac{4\sin^3\theta}{6\theta - 3\sin^3 2\theta} \right\}
$$

(4)

$$
\lambda'_l = \begin{cases} (0.14 + 1.55n - 0.93n^2 + 6.20\alpha - 16.67\alpha^2)\lambda_l, & 0 < n < 0.55, \quad 0.1 < \alpha \le 0.25 \\ (6.16 - 14.35n + 9.66n^2 + 3.22\alpha - 12.5\alpha^2)\lambda_l, & 0.55 \le n \le 0.82, \quad 0.1 < \alpha \le 0.25 \end{cases}
$$

(5)

$$
\theta = \frac{n' + 1.56 l'_l + 0.11 l_f + 0.20}{1.08 l'_l + 0.34 l_f + 0.38}
$$

(6)

where θ is the central angle corresponding to the concrete compression zone of specimens; r_s is the distance from the cross-section center of specimens to the cross-section center of the longitudinal reinforcement; r is the cross-section radius of the specimens; θ, r_s and r are all illustrated in Fig. 6; l_l is the characteristic value of longitudinal reinforcement, $l_l = A_s f_y / A_g f'_c$; A_s is the longitudinal reinforcement area; l'_l is the characteristic value of longitudinal reinforcement considering the effect of the pre-stressed CFRP strips and the axial load ratio of specimens; l_f is the characteristic value of the pre-stressed CFRP strips, $l_f = 2E_f t_f \varepsilon_f / D f'_c$; m, t_f, E_f, b_f, ε_{if}, f_{fu} and ε_f are the total number, calculated thickness, elastic modulus, width, initial strain, ultimate tensile stress, and ultimate strain of CFRP strips, respectively; s_f is the space between adjacent CFRP strips; $n' = N / f'_{cc} A_g$, f_{cc} is the strength of confined concrete, which can be calculated as follows (Bai 2011)

$$f'_{cc} = f'_c \left[1 + 3.7 \left(\frac{f_{il} + f_{el} + f_r}{f'_c} \right)^{0.8268} \right] \tag{7}$$

where f_{il} and f_{el} are separately the initial confined stress and the effective confined stress to core concrete provided by pre-stressed CFRP strips, f_r is the confined stress to core concrete provided by stirrups

$$f_{il} = \frac{2 m t_f E_f \varepsilon_{if} b_f}{D l} \tag{8}$$

$$f_{el} = \alpha_h \left(1 - \frac{s_f}{2D} \right)^2 \frac{2 t_f f_{fu}}{D} \tag{9}$$

$$f_r = \frac{f_y A_{ss1}}{s d_{cor}} \tag{10}$$

where α_h is the effective tensile strain coefficient of CFRP strips, which is defined as the ratio of actual ultimate tensile strain to the theoretical ultimate tensile strain. When the diameter of specimens is 300mm, α_h is 0.46, 0.60 and 0.65 corresponding to the pre-stress 0.10, 0.20 and 0.25 of CFRP strips, respectively (Bai 2011); A_{ss1} is the cross-section area of single stirrup; s is the stirrup spacing; d_{cor} is the diameter of the core concrete inside the stirrups.

3.4 The peak displacement Δ_m

Because the calculation is too complicated and the calculated results are quite discrete, Δ_m is commonly determined with the empirical method (Saiidi and Sozen 1979, Saatcioglu 1991). Through multiple nonlinear regression analysis of the experimental data with 1stOpt software, Δ_m can be calculated as follows

$$\Delta_m = \begin{cases} (3.62 + 4.37n - 4.67n^2 \\ - 24\alpha + 64\alpha^2) \Delta_y, & 0 < n < 0.55, \quad 0.1 < \alpha \le 0.25, \quad R = 0.9999 \\ (5.97 - 12.23n + 9.26n^2 \\ - 0.9\alpha + 12.67\alpha^2) \Delta_y, & 0.55 \le n \le 0.82, \quad 0.1 < \alpha \le 0.25, \quad R = 0.9999 \end{cases} \tag{11}$$

where R is the correlation coefficient in regression analysis.

3.5 Elastic stiffness K_1

The main purpose of elasto-plastic seismic response analysis is to study the performance of specimens in the plastic phase (Binici 2008). It can be seen from Fig. 4 that there is no obvious inflection point on backbone curves of the strengthened specimens before yield, so the backbone curves before yield can be simplified as a straight line from the origin to the yield point (segment OA in Fig. 5), and the elastic stiffness K_1 can be expressed as follows

$$K_1 = \frac{P_y}{\Delta_y} \tag{12}$$

3.6 Strengthening stiffness K_2

The strengthening curve is defined as the connection between yield load point and peak load point (segment AG in Fig. 5), the strengthening stiffness is expressed as

$$K_2 = \frac{P_m - P_y}{\Delta_m - \Delta_y} \tag{13}$$

3.7 Degradation stiffness K_3

The degradation curve is defined as the connection between peak load point and ultimate displacement point (segment GH in Fig. 5). The degradation stiffness of this segment is defined as $K_3 = \beta K_1$, where β is the stiffness degradation ratio of the degradation stiffness K_3 and the elastic stiffness K_1, and it can be calculated as Eq. (14). The stiffness degradation ratio β of the degradation segment is listed in Table 3, where K_{1t}, K_{3t} and β_t are calculated from the experimental data, β is calculated from Eq. (14).

$$K_3 = \begin{cases} (-0.33 + 0.29n - 0.68n^2 + 2.11\alpha - 4.94\alpha^2)K_1, & 0 < n < 0.55, \quad 0.1 < \alpha \le 0.25 \\ (-3.34 + 9.67n - 7.55n^2 + 1.61\alpha - 4.29\alpha^2)K_1, & 0.55 \le n \le 0.82, \quad 0.1 < \alpha \le 0.25 \end{cases} \tag{14}$$

Table 3 Stiffness degradation ratio β of degradation segment

Specimen	K_{1t} kN/mm	K_{3t} kN/mm	β_t	β	β / β_t
C3	25.23	-4.12	-0.1632	-0.1612	0.988
C4	26.13	-2.63	-0.1005	-0.0984	0.979
C5	25.08	-1.97	-0.0784	-0.0756	0.964
C6	28.03	-4.29	-0.1531	-0.1518	0.992
C8	26.98	-4.56	-0.1689	-0.1575	0.932
C10	27.63	-3.29	-0.1190	-0.1188	0.999
C11	26.39	-9.74	-0.3691	-0.3693	1.001
C12	25.67	-8.63	-0.3363	-0.3355	0.998

3.8 Unloading stiffness K_u

The stiffness of unloading segment (segment BC in Fig. 5) K_u can be calculated as follows. The degradation ratio ψ of unloading stiffness under different load cycles is listed in Table 4.

$$K_u = aK_1 \left(\frac{\Delta}{\Delta_y} \right)^b \tag{15}$$

$$a = \begin{cases} 0.79 + 0.43n - 0.06n^2 + 6.92\alpha - 25.83\alpha^2, & 0 < n < 0.55, & 0.1 < \alpha \le 0.25 \\ 5.36 - 13.3n + 9.1n^2 + 8.8\alpha - 30\alpha^2, & 0.55 \le n \le 0.82, & 0.1 < \alpha \le 0.25 \end{cases} \tag{16}$$

$$b = \begin{cases} 0.02 - 0.51n - 0.11n^2 - 6.23\alpha + 25.93\alpha^2, & 0 < n < 0.55, & 0.1 < \alpha \le 0.25 \\ -3.5 + 10.4n - 6.85n^2 - 10.1\alpha + 34.5\alpha^2, & 0.55 \le n \le 0.82, & 0.1 < \alpha \le 0.25 \end{cases} \tag{17}$$

where Δ is the horizontal displacement corresponding to the unloading point at the backbone curve.

3.9 The repeated loading path and strength degradation rate

It can be seen from Fig. 4 that there are apparent upper and lower intersection points on the hysteresis curves of strengthened specimens. The intersection point of the straight lines $P = 0.70P_y$ and $P = K_1\Delta$ can be taken as the upper intersection point based on the analysis of test results and its symmetric point about the origin as the lower one, respectively.

After yield load point, the reverse loading or re-loading path after unloading points to the lower intersection point (the upper intersection point) first, then points to the strength degradation point corresponding to the historical minimum (maximum) horizontal displacement point (Saiidi and Sozen 1979, Saatcioglu 1991).

Table 4 Stiffness degradation ratio ψ of unloading segment

specimen	Stiffness degradation ratio ψ					
	$2\Delta_y$ mm	$3\Delta_y$ mm	$3.5\Delta_y$ mm	$4\Delta_y$ mm	$4.5\Delta_y$ mm	$5\Delta_y$ mm
C3	0.9354	0.7530	0.6797	0.6341	—	—
C4	0.9710	0.8588	0.7693	0.7310	0.7210	0.6648
C5	0.9621	0.9147	0.8649	0.8023	0.7281	—
C6	0.9276	0.8534	0.0000	0.6457	—	—
C8	0.9372	0.9154	0.8620	0.7823	—	—
C9	0.8997	0.8315	0.8224	0.7470	—	—
C10	0.8848	0.8445	0.8026	0.7239	—	—
C11	0.9427	0.8370	—	—	—	—
C12	0.9514	0.8709	0.8416	—	—	—

Table 5 Strength degradation ratio γ

Specimen	Strength degradation ratio γ					
	$2\Delta_y$ mm	$3\Delta_y$ mm	$3.5\Delta_y$ mm	$4\Delta_y$ mm	$4.5\Delta_y$ mm	$5\Delta_y$ mm
C3	0.9789	0.8979	0.8679	0.8494	—	—
C4	0.9674	0.8969	0.8877	0.8812	0.8805	0.8132
C5	0.9196	0.9053	0.8870	0.8824	—	—
C6	0.9523	0.8980	0.7468	—	—	—
C8	0.9686	0.9255	0.9011	0.7965	—	—
C9	0.9325	0.9196	0.8162	—	—	—
C10	0.9454	0.9156	0.9031	—	—	—
C11	0.94633	0.6772	—	—	—	—
C12	0.9311	0.9128	—	—	—	—

The strength degradation rate γ is defined as the ratio of the maximum horizontal load in the third load cycle to the maximum horizontal load in the first load cycle at each control displacement. The values of γ under deferent horizontal displacement are shown in Table 5, which can be calculated as follows

$$\gamma = \begin{cases} -0.004e^{1.72n\mu} + 0.895e^{0.3\alpha}, & 0 < n < 0.55, \quad 0.1 < \alpha \le 0.25 \\ 1.08e^{-0.19n\mu} + 0.014e^{14.4n\alpha}, & 0.55 \le n \le 0.82, \quad 0.1 < \alpha \le 0.25 \end{cases} \tag{18}$$

where μ is the displacement ductility ratio, $\mu = \Delta_u / \Delta_y$; Δ_u is the ultimate displacement of specimen corresponding with the bearing capacity drops to 85% of the ultimate value.

3.10 Hysteresis rules

The hysteresis rules of restoring force model of circular RC columns strengthened by pre-stressed CFRP strips can be summed up as follows:

(1) The loading and unloading path both are along the elastic segment of the backbone curves (OA in Fig. 5) before yield.
(2) The loading path is along the backbone curves (AB and DE in Fig. 5) after yield. When unloading from the backbone curve (BC in Fig. 5), the unloading stiffness can be calculated with Eq. (15).
(3) The reverse loading or re-loading path points to the lower intersection point (the upper intersection point) first, then points to the strength degradation point corresponding to the historical minimum (maximum) horizontal displacement point (point J' and G' in Fig. 5), the strength degradation rate can be calculated by Eq. (18).
(4) The reverse loading path points to the lower intersection point first, and then points to the strength degradation point (point J' in Fig. 5) corresponding to the historical minimum horizontal displacement point (point E in Fig. 5). After reaching the backbone curve, it runs along the backbone curve (JK in Fig. 5).

## 4. Comparison of recommended model predictions with experimental results

As seen from Table 6, comparison between the calculated and experimental results for the main performance points on the backbone curves of circular RC columns strengthened by pre-stressed CFRP strips, which shows that they are predicted with satisfactory accuracy. In Table 6, P_{yt} and P_y are the experimental and calculated value of yield load, Δ_{yt} and Δ_y are the experimental and calculated value of yield displacement, P_{mt} and P_m are the experimental and calculated value of peak load, Δ_{mt} and Δ_m are the experimental and calculated value of peak displacement, respectively.

For the yield load P_y, yield displacement Δ_y, peak load P_m and peak displacement Δ_m, the differences between the proposed model and experimental results are not more than 5%.

The backbone curves were obtained from the proposed model as shown in Fig. 7, where the abbreviation Cac. refers to the predicted tri-linear restoring force curves using the recommended model and Exp. means the experimental restoring force curves. The comparisons show that the proposed model predicts the performance in a satisfactory manner.

Table 6 Comparison of calculated and test results for main performance points

Specimen	P_{yt} kN	P_y kN	$\dfrac{P_{yt}}{P_y}$	Δ_{yt} mm	Δ_y mm	$\dfrac{\Delta_{yt}}{\Delta_y}$	P_{mt} kN	P_m kN	$\dfrac{P_{mt}}{P_m}$	Δ_{mt} mm	Δ_m mm	$\dfrac{\Delta_{mt}}{\Delta_m}$
C3	164	157.9	1.039	6.50	6.30	1.032	210.0	201.0	1.045	18.60	18.02	1.032
C4	162	158.2	1.024	6.20	6.30	0.984	227.3	217.6	1.045	14.77	15.00	0.985
C5	158	154.8	1.021	6.30	6.30	1.000	194.1	188.0	1.032	13.73	13.74	0.999
C6	185	180.8	1.023	6.60	6.30	1.048	247.1	235.3	1.050	15.61	14.94	1.045
C8	170	166.0	1.024	6.30	6.30	1.000	235.2	229.2	1.026	16.47	16.45	1.001
C9	166	161.6	1.027	6.20	6.13	1.011	207.1	202.31	1.024	19.68	—	—
C10	163	156.1	1.044	5.90	6.13	0.962	210.8	205.69	1.025	13.49	13.52	0.998
C11	161	155.0	1.038	6.10	6.13	0.995	218.2	213.83	1.020	14.05	14.04	1.001
C12	154	149.9	1.027	6.00	6.13	0.979	213.1	208.53	1.022	15.52	15.55	0.998
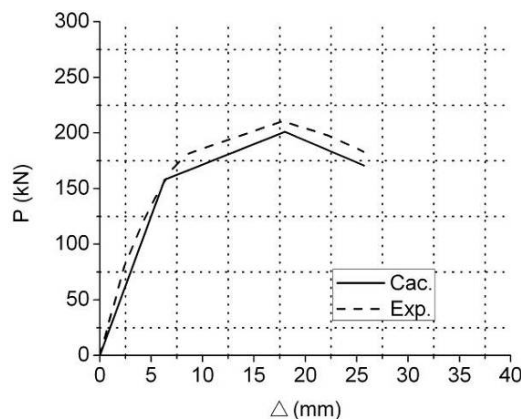
(a) C3
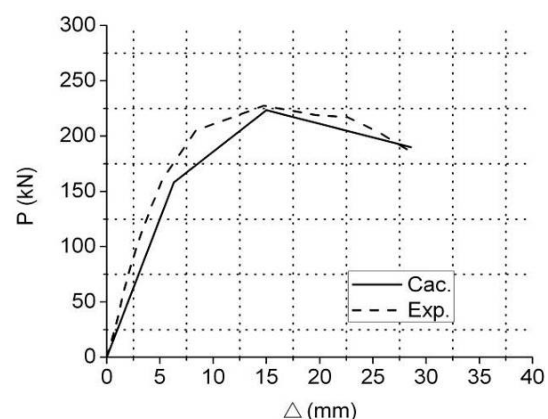
(b) C4

Fig. 7 Comparison of backbone curves between the proposed model and experimental results

(c) C5

(d) C6

(e) C8

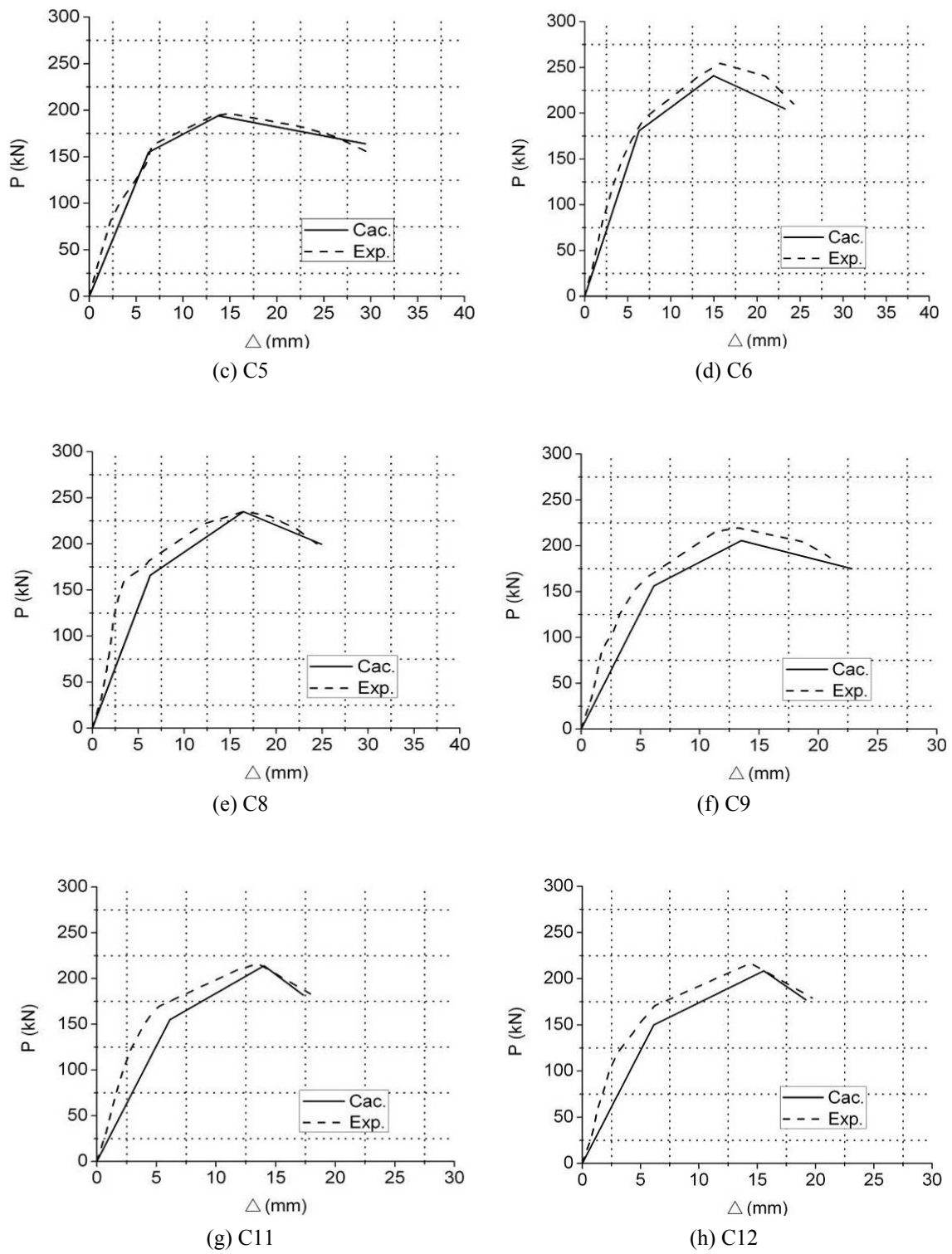(f) C9

(g) C11

(h) C12

Fig. 7 Comparison of backbone curves between the proposed model and experimental results

5. Conclusions

A tri-linear restoring force to predict the seismic behavior of circular RC columns strengthened by pre-stressed CFRP strips was developed based on the experimental results of 12 specimens under low cyclic loading. Both the effects of the pre-stress of CFRP strips and the axial load ratio are considered in the proposed model. The yield load, yield displacement, peak load, peak displacement and the backbone curves predicted from the proposed model are all in good agreement with experimental results.

Acknowledgments

References

ACI (2008), "Guide for the design and construction of externally bonded FRP systems for strengthening concrete structures", ACI 440.2R-08, American Concrete Institute, Farmington Hills, MI, USA.

Bai, X.B. (2011), "Study on the performance of circular concrete columns confined with lateral pre-tensioned FRP under axial load", Beijing Jiaotong University, Beijing, China. [In Chinese]

Binici, B. (2008), "Design of FRPs in circular bridge column retrofits for ductility enhancement", *Eng. Struct.*, **30**(3), 766-776.

Burt, K. and Aftab, A. (1999), "Investigation of the behavior of circular concrete columns reinforced with carbon fiber reinforced polymer (CFRP) jackets", *Can. J. Civil Eng.*, **26**(5), 590-596

CEB-FIP (CEB-FIP model code) (1990), *Comite Euro-International Du Beton*, Thomas Telford, London, UK.

FIB (2001), "Externally bonded FRP reinforcement for RC structures", *Proceedings of the 14th International Federation for Structural Concrete*, Technical report, Bulletin No. 14.

Gu, D.S., Wu, G. and Wu, Z.S. (2010), "Ultimate flexural strength of normal section of FRP-confined RC circular columns", *J. Southeast Univ.* (English Edition), **26**(1), 107-111.

Ibarra, L.F., Medina, R.A. and Krawinkler, H. (2005), "Hysteretic models that incorporate strength and stiffness deterioration", *Earthq. Eng. Struct. Dyn.*, **34**(12), 1489-1511.

ISIS (2001), "Strengthening reinforced concrete structures with externally bonded fiber reinforced polymers", The Canadian Network of Centers of Excellence on Intelligent Sensing for Innovative Structures, Canada.

JSCE (2001), "Recommendations for upgrading of concrete structures with use of continuous fiber sheets", Concrete engineering, Series 41, Japanese Society of Civil Engineers, Tokyo, Japan.

National Standard of the People's Republic of China (2002), "GB/T 50081-2002: Standard for test method of mechanical properties on ordinary concrete", China Building Industry Press, Beijing, China.

Nesheli, K.N. and Meguro, K. (2006), "Seismic retrofitting of earthquake-damaged concrete columns by lateral pre-tensioning of FRP belts", *Proceedings of the 8th U.S. National Conference on Earthquake Engineering*, San Francisco, CA, USA, April.

Saatcioglu, M. (1991), "Modeling hysteretic force-deformation relationships for reinforced concrete elements", Special Publication, **127**(5), 153-198.

Saiidi, M. and Sozen, M.A. (1979), "Simple and complex models for nonlinear seismic response of reinforced concrete structures", Ph.D. Thesis, Structural Research Series 465, Civil Engineering Studies, University of Illinois Engineering Experiment Station, College of Engineering, University of Illinois at Urbana-Champaign, Urbana, IL, USA.

Sheikh, S. (2001), "Use of FRP composites for seismic upgrade of concrete columns", *Proceedings of the International Conference on FRP Composites in Civil Engineering*, Hong Kong, December.

Sheikh, S.A. (2002), "Performance of concrete structures retrofitted with fibre reinforced polymers", *Eng. Struct.*, **24**(7), 869-879.

Sivaselvan, M.V. and Reinhorn, A.M. (2000), "Hysteretic models for deteriorating inelastic structures", *J. Eng. Mech.*, **126**(6), 633-640.

Stojadinovic, B. and Thewalt, C. (1996), "Energy balanced hysteresis models", *Proceedings of the 11th World Conference on Earthquake Engineering*, Acapulco, Mexico, June.

Stone, W.C. and Taylor, A.W. (1992), "A predictive model for hysteretic failure parameters", *Proceedings of the 10th World Conference on Earthquake Engineering*, Madrid, Spain, July.

Su, X.Z. (1998), "Study on seismic resistance of the prestressed concrete frame structure", Shanghai Science and Technology Press, 118-119, Shanghai, China. [In Chinese]

Taleie, S.M. and Moghaddam, H. (2007), "Experimental and analytical investigation of square RC columns retrofitted with pre-stressed FRP strips", *Proceedings of the 8th International Symposium on FRP Reinforcement for Concrete Structures*, Patras, Greece.

Taleie, S.M. and Oskouei, A.V. (2007), "Experimental investigation of FRP relaxation and its effect on pre-stressing techniques", *Proceedings of the 8th International Symposium on FRP Reinforcement for Concrete Structures*, Patras, Greece.

Tamai, S., Sato, T. and Okamoto, M. (2000), "Hysteresis model of steel jacketed RC columns for railway viaducts", IABSE Congress Report.

Tao, Z., Gao, X. and Yu, Q. (2005), "Theoretical analysis of hysteretic behavior of FRP-confined RC columns", *Indust. Construct.*, **35**(9), 15-19. [In Chinese]

Teng, J.G., Chen, J., Smith, S. and Lam, L. (2002), *FRP: Strengthened RC Structures*, John Wiley & Sons.

Xiao, Y. and Ma, R. (1997), "Seismic retrofit of RC circular columns using prefabricated composite jacketing", *J. Struct. Eng.*, **123**(10), 1357-1364.

Yamakawa, T., Nesheli, K.N. and Satoh, H. (2001), "Seismic or emergency retrofit of RC short columns by use of prestressed aramid fiber belts as external hoops", *J. Struct. Construct. Eng.*, **550**, 135-141.

CC